# Density-dependent changes of the pore properties of the $P2X_2$ receptor channel

Yuichiro Fujiwara[1,2] and Yoshihiro Kubo[1,2,3]

[1]*Department of Physiology and Cell Biology, COE Program for Brain Integration and its Disorders, Tokyo Medical and Dental University Graduate School and Faculty of Medicine, Tokyo 113-8519, Japan*
[2]*Division of Biophysics and Neurobiology, Department of Molecular Physiology, National Institute for Physiological Sciences, Aichi 444-8585, Japan*
[3]*CREST, Japan Science and Technology Corporation, Saitama 332-0012, Japan*

**Ligand-gated ion channels underlie and play important roles in synaptic transmission, and it is generally accepted that the ion channel pores have a rigid structure that enables strict regulation of ion permeation. One exception is the P2X ATP-gated channel. After application of ATP, the ion selectivity of the $P2X_2$ channel time-dependently changes, i.e. permeability to large cations gradually increases, and there is significant cell-to-cell variation in the intensity of inward rectification. Here we show $P2X_2$ channel properties are correlated with the expression level: increasing $P2X_2$ expression level in oocytes increases permeability to large cations, decreases inward rectification and increases ligand sensitivity. We also observed that the inward rectification changed in a dose-dependent manner, i.e. when low concentration of ATP was applied to an oocyte with a high expression level, the intensity of inward rectification of the evoked current was weak. Taken together, these results show that the pore properties of $P2X_2$ channel are not static but change dynamically depending on the open channel density. Furthermore, we identified by mutagenesis study that Ile328 located at the outer mouth of the pore is critical for the density-dependent changes of $P2X_2$. Our findings suggest synaptic transmission can be modulated by the local density-dependent changes of channel properties caused, for example, by the presence of clustering molecules.**

(Resubmitted 15 March 2004; accepted after revision 20 April 2004; first published online 23 April 2004)
**Corresponding author** Y. Kubo: Division of Biophysics and Neurobiology, Department of Molecular Physiology, National Institute for Physiological Sciences, Aichi 444-8585, Japan. Email: ykubo@nips.ac.jp

P2X receptors are ATP-gated ion channels that are widely distributed in the peripheral and central nervous system. They are non-selective cation channels (Virginio *et al.* 1999) with the property of inward rectification (Khakh *et al.* 1995; Evans *et al.* 1996; Zhou & Hume, 1998). It is known that they play critical roles in fast synaptic transmission (Edwards *et al.* 1992; Evans *et al.* 1992) and in presynaptic modulation (Gu & MacDermott, 1997; Khakh & Henderson, 1998; Kato & Shigetomi, 2001).

The primary structure of P2X receptors was determined by the isolation of the first cDNA by the expression cloning method (Brake *et al.* 1994; Valera *et al.* 1994), and seven types of P2X cDNAs have been cloned so far (North & Barnard, 1997; North, 2002). All of them have two transmembrane regions with a large extracellular loop, and the functional unit is reported to be composed of three subunits based on the analysis of the weight of the non-denatured proteins (Nicke *et al.* 1998). This structure, a trimer of two transmembrane type subunits, is in clear contrast with other ligand-gated channels such as nicotinic acetylcholine (nACh) receptors or glutamate receptors (Khakh, 2001), suggesting the possibility of functional differences.

The P2X receptor channel is unique not only from a structural but also from a functional point of view. First, its ion selectivity changes dynamically within a time frame measured in seconds (Surprenant *et al.* 1996; Khakh & Lester, 1999; Virginio *et al.* 1999; Khakh *et al.* 2001; Eickhorst *et al.* 2002), i.e. only small cations such as $Na^+$ and $K^+$ can pass through the channel pore early after ATP application, but cations as large as *N*-methyl-D-glucamine (NMDG) pass through the channel later (Virginio *et al.* 1999; Eickhorst *et al.* 2002). Second, there is a significant cell-to-cell variation in the intensity of the inward rectification through the $P2X_2$ channel (Khakh *et al.* 1995; Evans *et al.* 1996). Third, the channels interact with nACh receptors directly on the membrane, resulting

 DOI: 10.1113/jphysiol.2004.064568

in inhibition of the nACh receptor current (Nakazawa, 1994; Khakh *et al.* 2000).

As it is generally accepted that pore properties of ion channels such as ion selectivity and rectification are determined strictly by the tight molecular base like those of KcsA (Doyle *et al.* 1998; Zhou *et al.* 2001) or Kir (Nichols & Lopatin, 1997; Kubo & Murata, 2001; Fujiwara & Kubo, 2002; Nishida & MacKinnon, 2002), the three unique properties of P2X receptors, which account for the dynamics and flexibility of the pore, are all the more noteworthy.

We initially aimed to identify structural determinants of $P2X_2$ receptors involved in the property of inward rectification and prepared various mutants. However, reliable determination of the mutant phenotype was hard, because the intensity of inward rectification varied significantly even in the wild-type (WT). We later noticed that the variation of the inward rectification intensity was due to a difference in expression level. Khakh *et al.* (2000) also reported the significance of the expression level for the functional interaction between $P2X_2$ and nACH receptors. Triggered by these observations, we decided to focus on the correlation of the expression density and the channel properties of the $P2X_2$ receptor. In the present study, we used *Xenopus* oocytes as an expression system, and analysed channel properties such as the ion selectivity, inward rectification and ATP sensitivity by recording ATP-evoked current under two-electrode voltage clamp from oocytes with various express levels.

## Methods

### Molecular biology

A *Bam*H1–*Not*1 fragment of the original rat $P2X_2$ receptor cDNA (Brake *et al.* 1994) was subcloned into pBluescript vector. cRNA was then prepared from the linearized plasmid cDNA using an RNA transcription kit (Stratagene). The single point mutant was made with a QuickChange site-directed mutagenesis kit (Stratagene) and confirmed by sequencing.

### Preparation of *Xenopus* oocytes

*Xenopus* oocytes were collected from frogs anaesthetized in water containing 0.15% tricaine; after the final collection the frogs were killed by decapitation. Isolated oocytes were treated with collagenase (2 mg $ml^{-1}$, type 1, Sigma), after which oocytes of similar size at stage V were injected with approximately 50 nl of cRNA solution. Serial dilutions (1 : 1 to 1 : 1000) of the cRNA in water enabled induction of various levels of $P2X_2$ receptor expression. The injected oocytes were incubated for 1–2 days at 17°C in frog Ringer solution.

All experiments conformed with the guidelines of the Animal care Committees of Tokyo Medical and Dental University and the National Institute for Physiological Sciences.

### Electrophysiology

Macroscopic currents were recorded using the two-electrode voltage clamp technique with a bath-clamp amplifier (OC-725C, Warner Instruments, Inc., Hamden, CT, USA). Stimulation, data acquisition and data analysis were all done on a Pentium-based computer using Digidata 1322A and pCLAMP 8.2 software (Axon Instruments, Union City, CA, USA). All recordings were obtained at room temperature (20–23°C). Intracellular glass microelectrodes were filled with 3 M potassium acetate with 10 mM KCl (pH 7.2). The microelectrode resistances ranged from 0.1 to 0.3 MΩ. Two Ag–AgCl pellets (Warner Instruments) were used to pass the bath current and sense the bath voltage. The voltage-sensing electrode was placed near the oocyte (approximately 2 mm away) on the same side as the voltage-recording microelectrode. The bath current-passing pellet and the current injection microelectrode were placed on the other side.

The recording bath solution contained 98 mM NaCl, 1 mM $MgCl_2$ and 5 mM Hepes (pH 7.35–7.40). For the experiment on the permeability of NMDG and $K^+$ in Figs 1 and 2, the bath solution contained 98 mM NMDG, 85 mM HCl, 1 mM $MgCl_2$ and 5 mM Hepes (pH 7.35–7.40), or 98 mM KCl, 1 mM $MgCl_2$ and 5 mM Hepes (pH 7.35–7.40). $Ca^{2+}$ was not included in the bath solution to avoid channel desensitization and a variety of secondary intracellular effects. ATP disodium salt (Sigma) was dissolved in bath solution just before each experiment. When applied to cells, one-fifth bath volume of 5 times concentrated solution was pipetted into the bath; complete exchange of solution around the oocyte was confirmed within ∼0.5 s.

Current–voltage relationships were recorded at steady states (at ∼5 s after ATP application) by applying slow ramp pulses from −75 to +75 mV over 1.5 s (Figs 1*D–F*, 3*A–E*, 5*A–C*, and 6*A*, *B* and *D*), reverse ramp pulses from +75 mV to −75 mV over 1.5 s (Fig. 3*F*), and ramp pulses from −105 to 75 mV over 1.8 s (Fig. 1*A–C*). Reversal potentials in Fig. 2 were recorded by applying 360 ms ramp pulses from −105 to 0 mV repeatedly every 500 ms for 30 s after ATP application. The data in Fig. 4 were recorded by applying a set of step pulses at a steady state (at ∼5 s after ATP application); cells were held at 0 mV, then stepped to

−80 mV for 150 ms, after which 300-ms test pulses from +60 to −30 mV were applied in 10 mV decrements. All recorded currents, except for those of I328F mutants which showed a basally active component, were leak subtracted, i.e. the background leak current before ATP application was subtracted from the ATP-evoked current. The leak current was monitored again after washing out the ATP, and records showing a significant increase in leak current were discarded. Actual clamped membrane potentials were monitored during the recordings, and data with an error of over 2 mV from the command potentials were discarded (Kubo & Murata, 2001; Fujiwara & Kubo, 2002).

### Data analysis

Data were analysed using Clampfit 8 (Axon Instruments, Inc) or Igor Pro (WaveMetrics, Inc., Lake Oswego, OR, USA). Ion permeability ratios in Figs 1*C* and *F* and 2*C* were calculated from the shift of the reversal potential using the function $P_X/P_Y = \exp(\Delta E_{rev}F/RT)$, where $\Delta E_{rev}$ is the difference of the reversal potentials between $E_{rev,X}$ and $E_{rev,Y}$ (Khakh *et al.* 1999). As an index of the intensity of inward rectification in Figs 3*C–F*, 5*C* and 6*A* and *D* the ratio of the current amplitudes at +40 mV and −60 mV was calculated. Decaying outward currents in Figs 4*A* and *D* could be fitted satisfactorily with a single exponential function, and the fitting qualities were not improved by fitting with a double exponential function. $K_d$ and the Hill coefficient in Figs 5 and 6 were calculated from the current amplitudes at a steady state in $Na^+$-based external solution at −60 mV obtained by applying various [ATP] by fitting the [ATP]–response relationship with the Hill equation. Correlations of two parameters were calculated by simple linear regression; the regression lines and the correlation coefficients are shown on the graphs. Two regression groups were compared statistically using their regression slopes in Figs 3*D* and 6*A* and *D*. Data from the same batch of oocytes were used for comparison of phenotypes because properties such as the inward rectification differed from batch to batch. Nevertheless, similar tendencies were reproducibly observed in 11 batches of oocytes.

## Results

### Correlative changes of the ion selectivity with the expression level

We have observed that the extent of the change in ion selectivity correlates with the level of the channel's expression. After establishing a two-electrode voltage clamp configuration, we applied a saturating concentration (100 $\mu$M) of ATP to oocytes expressing low (Fig. 1*A*) or high (Fig. 1*B*) levels of $P2X_2$ in $Na^+$-based or NMDG-based external solution. We obtained current–voltage (*I–V*) relationships by applying slow (1.8 s) ramp pulses after 8 s of ATP application (Figs 1*A* and *B*). In an oocyte with a high expression level the value of the reversal potential in NMDG-based external solution was more depolarized than that in an oocyte with a low expression level, indicative of higher NMDG permeability (Figs 1*A* and *B*). $P_{NMDG}/P_{Na}$ ratios at 8 s showed a positive correlation with the expression level (Fig. 1*C*). We performed the same recording in oocytes expressing low (Fig. 1*D*) or high (Fig. 1*E*) levels of $P2X_2$ in $Na^+$-based or $K^+$-based external solution. $P_K/P_{Na}$ ratios showed no correlation with the expression level (Fig. 1*F*). We also found that the inward rectification in oocytes expressing a high level of $P2X_2$ was weaker than that in those expressing a low level (Fig. 1*A* and *B*, or *D* and *E*), and this is analysed further in the next section.

Next we examined whether or not the time-dependent change of permeability to NMDG was dependent on the expression level. By applying ramp pulses repeatedly, we observed that there was a time-dependent shift in the reversal potential toward depolarization in NMDG-based solution that was much more pronounced in cells expressing high levels of $P2X_2$ (Fig. 2*A*). Changes of reversal potentials in Fig. 2*A* are shown in Fig. 2*B*. The calculated permeability ratios of NMDG and $Na^+$ ($P_{NMDG}/P_{Na}$) at 3 s, 10 s and 25 s after ATP application were all positively correlated with the inward current amplitude (Fig. 2*C*). In short, $P2X_2$ channels showed low permeability to NMDG immediately after application of ATP even when the expression level was high. The permeability to NMDG increased depending on time and the increase was notable when the expression level was high.

Time-dependent increase in NMDG permeation was reported previously for $P2X_7$ (Surprenant *et al.* 1996) and $P2X_2$ (Virginio *et al.* 1999; Eickhorst *et al.* 2002), and it was shown that the changes are not due to ion flux. The novel finding of the present work is that the change is more prominent when the expression level is high. As we used a similar recording condition to the previous studies, we think the time-dependent changes are not due to ion flux.

### Correlation between the inward rectification intensity and the expression level

We next investigated the relationships between the inward rectification intensity of $P2X_2$ and the expression level. Current traces were obtained from oocytes expressing

various levels of $P2X_2$ by applying ramp pulses while the cells were in a steady state after application of 100 $\mu$M ATP in $Na^+$-based external solution (Fig. 3*A*). The normalized *I–V* relationships showed that the intensity of the inward rectification varied from cell to cell (Fig. 3*B*). When the accumulated data were plotted, the rectification index ($I_{+40\ mV}/I_{-60\ mV}$) showed a positive correlation with the inward current amplitude (Fig. 3*C*). This tendency was also observed in $K^+$-based external solution (Fig. 3*D*). In addition, there were no significant differences between two lines calculated by simple linear regression with the data in $Na^+$-based external solution and in $K^+$-based external solution.

In these experiments we induced variation in the level of $P2X_2$ expression by injecting oocytes with different amounts of cRNA. To confirm that the amount of injected cRNA did not influence the intensity of rectification, we analysed the correlation by recording from oocytes injected with the same amount of cRNA at various times after injection (Fig. 3*E*). In this experiment, the rectification index again correlated positively with the expression level (Fig. 3*E*), showing that the variation in rectification was not dependent on the injected amount of cRNA.

We also applied reverse ramp pulses in order to confirm that the intensity of rectification was not dependent on pulse protocols or ion fluxes as shown in Fig. 3*F*. We confirmed furthermore that ion fluxes could not affect the density-dependent change of inward rectification using rapid ramp pulses (360 ms), which minimize the ion flux, and frequently repeated ramp pulses (10 pulses during 15 s), which maximize it (data not shown). Taking these results together with those using $K^+$ as a charge carrier, and reverse or short or repetitive pulses, we concluded that the expression level-dependent changes of inward rectification intensity was not due to the ion flux but due to the expression level itself.

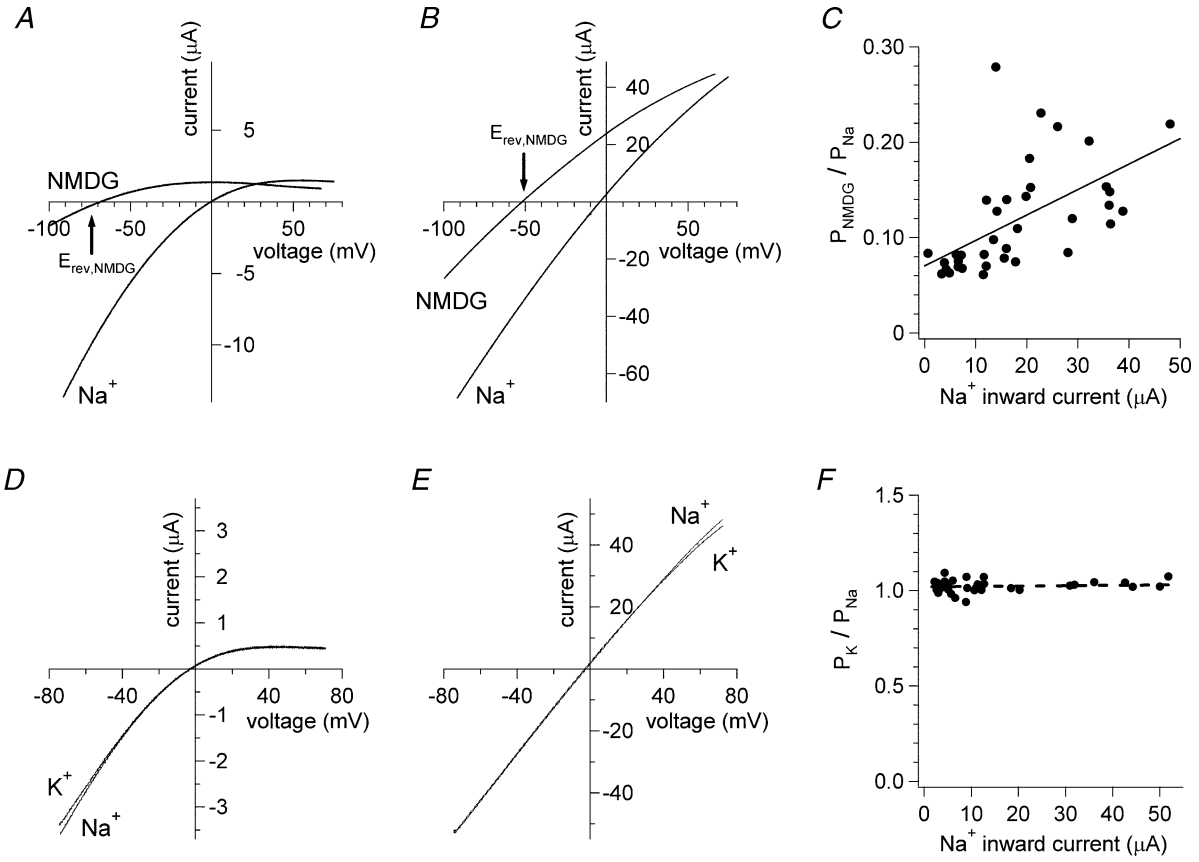


**Figure 1. Changes in the ion selectivity of the $P2X_2$ receptor channel were dependent on the receptor's expression level**

*A* and *B*, current–voltage relationships obtained 8 s after ATP application by applying ramp pulses to oocytes expressing low (*A*) or high (*B*) levels of $P2X_2$ receptor in $Na^+$-based or NMDG-based external solution. *C*, there was a positive correlation between $P_{NMDG}/P_{Na}$ and $P2X_2$ receptor expression level. *D* and *E*, current–voltage relationships were obtained from oocytes expressing low (*D*) or high (*E*) levels of $P2X_2$ receptor in $Na^+$-based or $K^+$-based external solution. *F*, there was no significant correlation between $P_K/P_{Na}$ and $P2X_2$ receptor expression.

### Analysis of the properties of the outward current and their correlation with the expression level

We analysed outward currents evoked by depolarizing step pulses at steady states after application of 100 $\mu$M ATP. Once inward currents elicited by application of 100 $\mu$M ATP reached a steady level, outward currents evoked by depolarizing step pulses showed a single exponential decay to a steady level. We measured the amplitudes of the inward current ($I_{inward}$ at −80 mV), the initial level at the beginning of the depolarizing pulses to +60 mV ($I_{initial}$) and the steady level at +60 mV ($I_{steady}$). The time constant of decay ($\tau$ at +60 mV) was calculated by fitting the trace with a single exponential function (Fig. 4*A*). We then analysed the correlations between these parameters and the inward current amplitude, i.e. the level of $P2X_2$ expression. $I_{initial}/I_{inward}$ (Fig. 4*B*, filled triangles with a continuous line), $I_{steady}/I_{inward}$ (Fig. 4*B*, open squares with a dotted line) and $I_{steady}/I_{initial}$ (Fig. 4*C*) all became larger as the level of $P2X_2$ expression was increased. $\tau$ remained virtually unchanged and showed no significant correlation with $P2X_2$ expression (Fig. 4*D*). Assuming that the current decay reflects the channel's transition from an open to a closed state, we calculated the rate constants between the two states. The rate constant for the transition to the closed state ($\alpha$) showed a negative correlation with the level of $P2X_2$ expression, while that for the transition to the open state ($\beta$) showed a positive correlation (Fig. 4*E*). The constant $\tau$-value reflects that the sum of $\alpha$ and $\beta$ remains constant. In summary, $\alpha$ and $\beta$ changed gradually in an opposite manner in accordance with the change in the expression level, keeping the sum constant. A similar tendency was observed at other potentials, ranging from +10 mV to +50 mV (not shown).

How can these expression level-dependent changes be explained? Here we propose two possible models, the 'gradual change model' and the 'mixed population model'. In the gradual change model, we assume that all channels at a given expression level have the same properties, and that the properties change gradually in a manner corresponding to the expression level. Although this model appears to explain the gradual changes of $\alpha$ and $\beta$ simply, it suffers from the unnatural assumption that the channel protein has an infinite number of functional states. Also, this model cannot explain well why the sum of $\alpha$ and $\beta$ remains constant. In the second model, the mixed population model, we assume the coexistence of two different types of channel, one with a decaying outward current and another with no decaying outward current. The observed outward currents reflect the sum of these

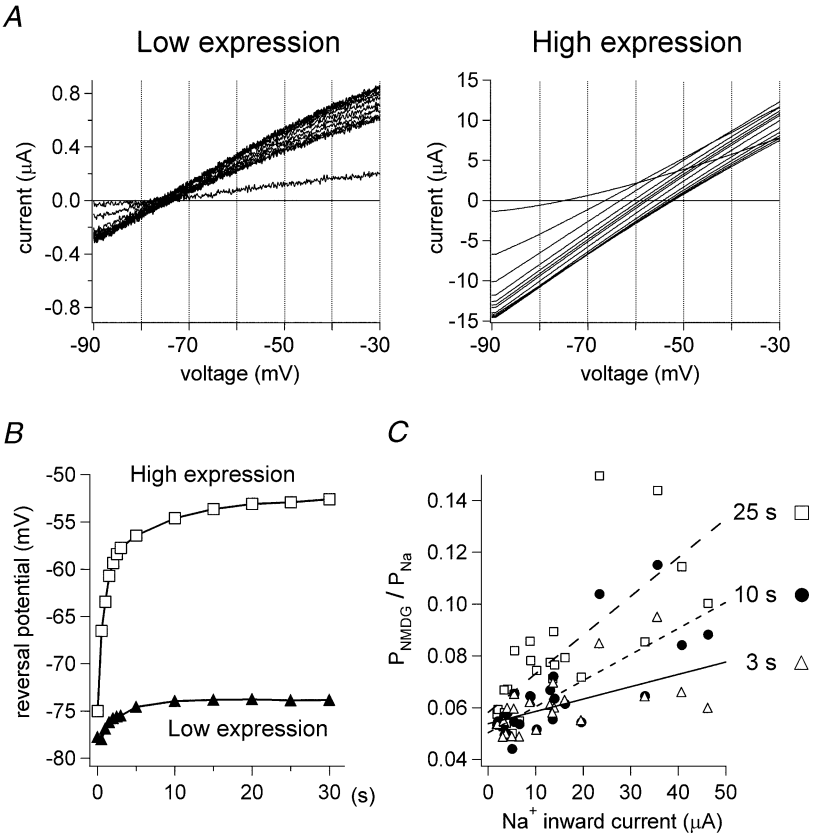


**Figure 2. The effect of the $P2X_2$ receptor's expression level on time-dependent increase in the permeability to NMDG**
*A*, current traces recorded 0.5, 1, 1.5, 2, 2.5, 3, 5, 10, 15, 20, 25 and 30 s after applying ATP to oocytes expressing low (left) and high (right) levels of $P2X_2$ receptor. *B*, time-dependent shifts of the reversal potentials were obtained from oocytes expressing low (▲) and high (□) levels of $P2X_2$. *C*, correlation between the expression level of $P2X_2$ receptor and $P_{NMDG}/P_{Na}$ at 3 s (Δ), 10 s (●) and 25 s (□) after ATP application. Calculated regression lines are also shown.

two components, and the fraction composed of the non-decaying type increases in accordance with the increases in the level of $P2X_2$ expression (Fig. 4*C*). This gradual increase in the fraction of non-decaying type explains the gradual decrease in $\alpha$, gradual increase in $\beta$ and constant sum of them. We think this second model is more natural and likely, but we have no conclusive evidence to exclude or to prove one of these two possibilities.

### Open channel density dependent dynamic changes of the inward rectification intensity

So far, we have shown that pore properties of $P2X_2$ change correlatively with the expression level. To test whether pore properties of expressed channels are static or can change dynamically, we compared the *I–V* relationships of currents induced by various concentration of ATP ([ATP]) in a single oocyte. Even in an identical oocyte with a high expression level, the intensity of rectification changed by applying various [ATP], i.e. low [ATP] induced a current exhibiting strong inward rectification (Fig. 5*A* and *B*). Accumulated data showed that the tendency was applicable at all expression levels (Fig. 5*C*). Taken together, the rectification intensity is correlated with the density of the 'open' channels, rather than with the density of all the channels expressed, i.e. even in an individual oocyte the pore properties of $P2X_2$ channels expressed were not stable and could be modified dynamically by applying various [ATP].

These results, however, might be explained also by assuming the presence of two static types of channel: a strong rectifier with high ligand sensitivity and a weak

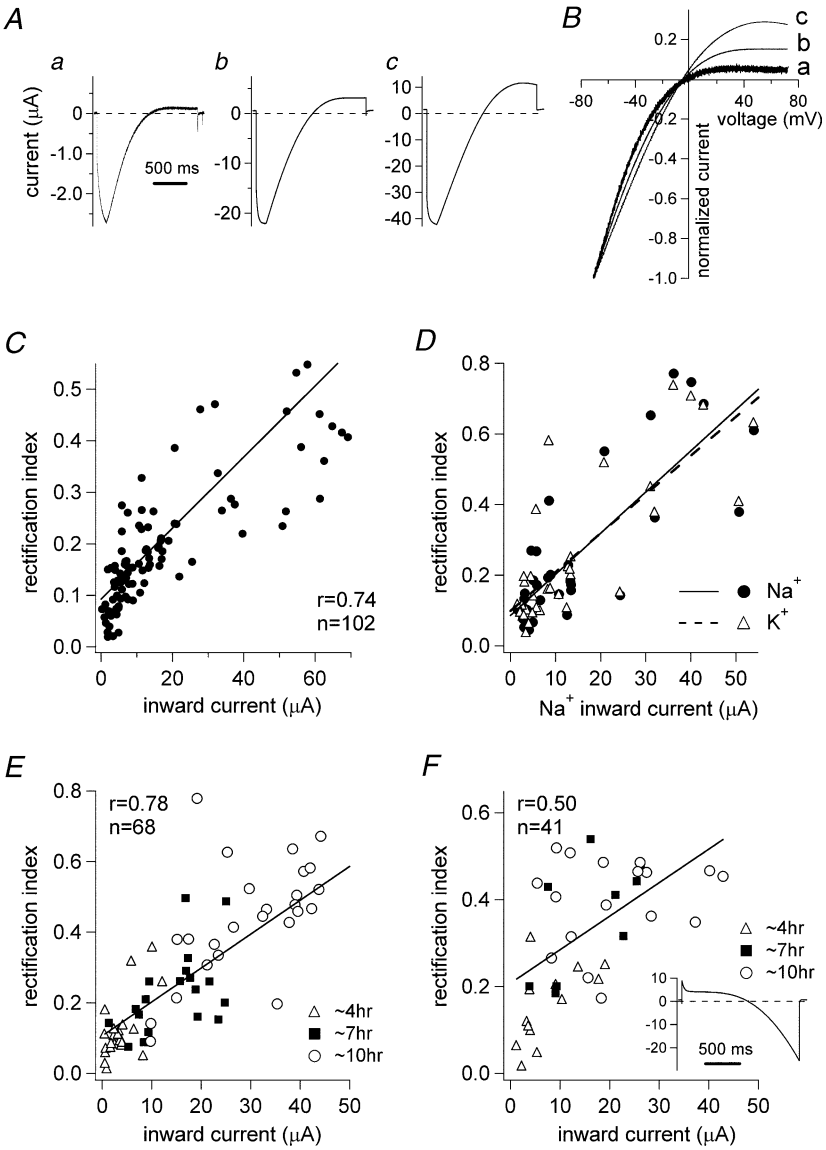


**Figure 3. Correlation between the intensity of the inward rectification of $P2X_2$ channel currents and the level of $P2X_2$ receptor expression**

*A*, representative currents recorded from oocytes expressing low (*a*), medium (*b*) and high (c) levels of $P2X_2$ receptor. *B*, normalized *I–V* relationships. *C*, correlation between the rectification index ($I_{+40\ mV}/I_{-60\ mV}$) and the current amplitude. *D*, same as in *C*, but in this case data obtained in $Na^+$-based and $K^+$-based external solution were compared. *E*, same as in *C*, except that recordings were obtained at various times after injecting the same amount of cRNA into oocytes. *F*, same as in *E*, except that reverse ramp pulses from depolarized to hyperpolarized potentials were applied.

rectifier with low ligand sensitivity. In that case, it is not necessary to assume dynamic changes in the open channel properties. To test this possibility we analysed the relationship between ligand sensitivity and the level of $P2X_2$ expression. Representative concentration–response relationships recorded from four oocytes with various expression levels were shown, and symbols connected by fitted curves are data from the same oocyte (Fig. 5*D*). The $K_d$ value for ATP, determined from the current amplitudes measured at a steady-state in $Na^+$-based solution, declined as the level of $P2X_2$ expression increased (Fig. 5*E*), though the Hill coefficient remained constant at ∼2 (Fig. 5*F*), which is similar to the recently reported findings of Clyne *et al.* (2003). The result that the weak rectifiers present at high expression levels showed a high ligand sensitivity is contrary to the assumption at the beginning of this paragraph. Instead, the results summarized in Fig. 7 can be most naturally explained by assuming that the pore

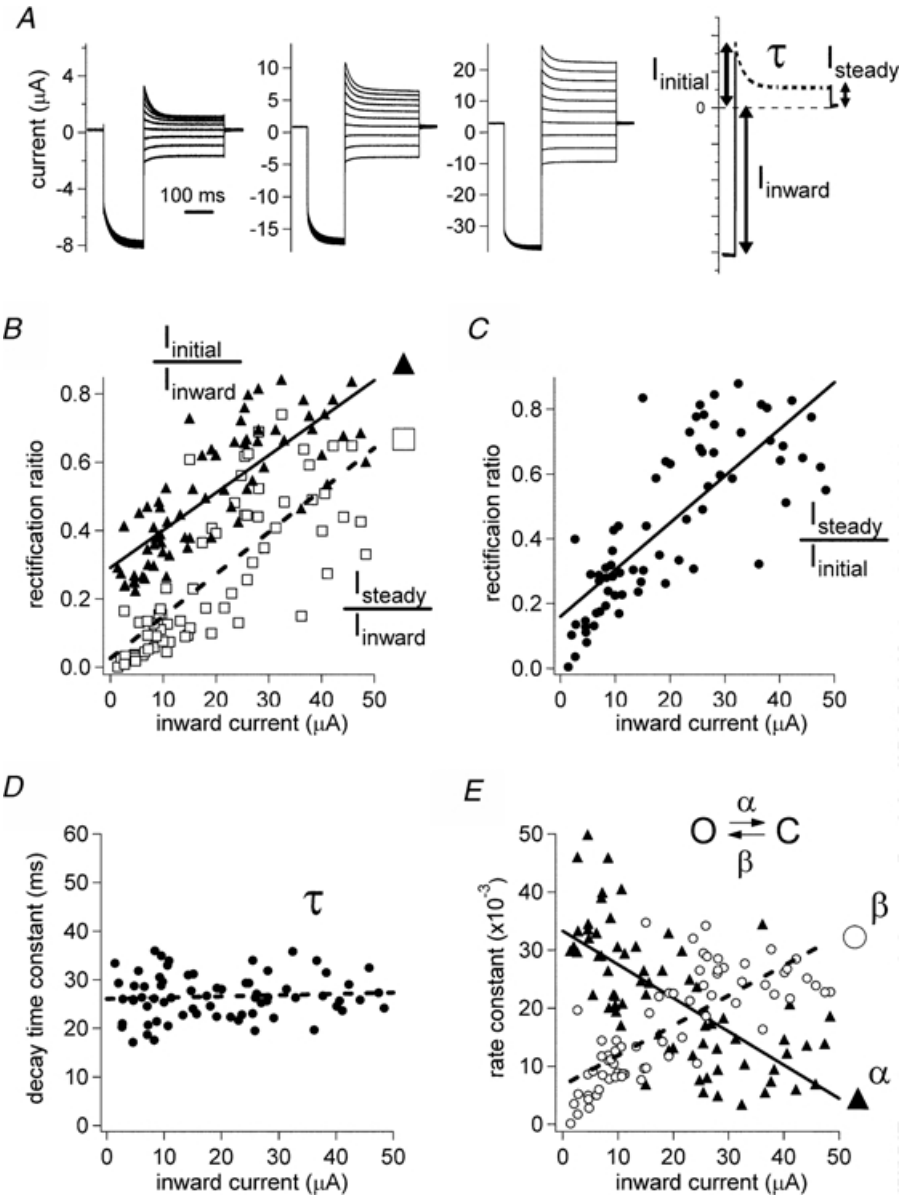


**Figure 4. Analysis of the properties of the outward current through the $P2X_2$ channel**
*A*, representative currents evoked by applying step pulses to oocytes showing increasing (left to right) levels of $P2X_2$ receptor expression; $I_{inward}$, $I_{initial}$, $I_{steady}$ and $\tau$ are defined schematically on the right. *B*, correlation between $I_{initial}/I_{inward}$ and $I_{inward}$ and between $I_{steady}/I_{inward}$ and $I_{inward}$. The lines were calculated by simple linear regression (also in *C*, *D* and *E*). *C*, correlation between $I_{steady}/I_{initial}$ and $I_{inward}$. *D*, correlation between $\tau$ and $I_{inward}$. *E*, correlation between calculated $\alpha$, $\beta$ and $I_{inward}$. $\alpha$ and $\beta$ were calculated from the two equations: $I_{steady}/I_{initial} = \beta/(\alpha + \beta)$, $\tau = 1/(\alpha + \beta)$.

properties change dynamically depending on the density of the open channels. Perhaps open channels situated in close proximity interact with one another, leading to a change in the pore properties.

### Structural determinant of the density-dependent changes of channel properties

To discover the structural determinant of density dependency, we tried to identify a point mutant whose

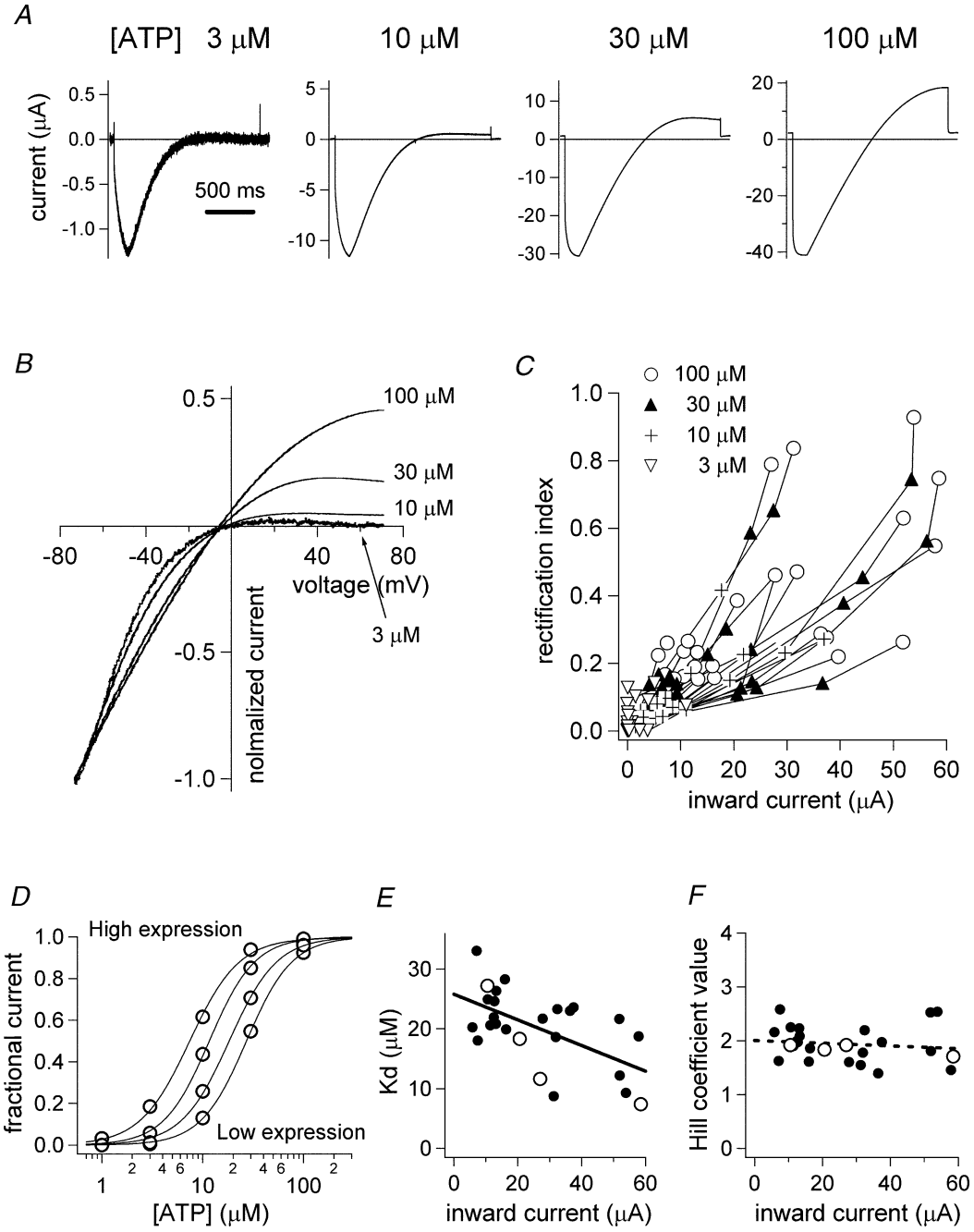


**Figure 5. Dependency of the inward rectification intensity on the open channel density**
*A*, representative current recordings evoked by applying ramp pulses to a single oocyte in the presence of various [ATP]. *B*, normalized *I–V* relationships. *C*, accumulated data showing the correlation of the rectification index with the current amplitude evoked by various [ATP]. Symbols connected by lines are data from the same oocyte. *D*, representative concentration–response relationships fitted with Hill equation. *E*, correlation between $K_d$ and the expression level. The data in *D* were plotted with open circles (also in *F*). *F*, there was no correlation between the Hill coefficient and the expression level.

rectification property does not clearly change depending on the channel density. As the change of the rectification property is expected to involve conformational changes of the pore, we introduced single point mutations systematically to the pore region, and identified I328 as a critical site. I328 is an amino acid residue conserved among all the P2X family and located just above the second transmembrane region; it has been reported by substituted cysteine accessibility analysis to contribute to the permeation pathway and to move during channel opening (Rassendren *et al.* 1997; Egan *et al.* 1998; Jiang *et al.* 2001). The correlation between the current amplitude and the rectification index ($I_{+40\ \mathrm{mV}}/I_{-60\ \mathrm{mV}}$) of the I328C mutant was compared with that of WT (Fig. 6*A*). I328C showed weaker inward rectification (i.e. a higher rectification index) than WT even in oocytes with a low expression level, and the slope of the regression line of the correlation was significantly less steep than that of WT ($P < 0.001$) (Fig. 6*A*). In an identical oocyte expressing I328C, the decrease in the rectification index by applying lower [ATP], which was observed in WT, was not remarkable (Fig. 6*B*). We also analysed the correlation between the $K_d$ value of [ATP] and the expression level (i.e. the inward current amplitude evoked by 100 $\mu$M ATP) and observed that the dependency was not apparent in the I328C mutant (Fig. 6*C*). Taken together, the dependency of both the inward rectification index and the $K_d$ value on the expression level was less clear in I328C than in WT.

We also made I328A, I328L and I328F mutants, and examined their inward rectification property. The slope of the regression line of I328A ($P < 0.001$), but not of I328L ($P > 0.05$), was significantly less steep than that of WT (Fig. 6*D*). In the case of the I328F mutant, we could not obtain reliable data for large amplitudes over 40 $\mu$A, because there was a large basally active component on top of the ATP-evoked current. In the obtained data range, the inward rectification intensity of I328F did not show a clear correlation with the current amplitude (Fig. 6*D*). In summary, the dependency of the inward rectification index on the expression level was affected not only in I328C but also in I328A and possibly in I328F, showing that this residue is critical.

## Discussion

In this study we analysed the variation of the properties of $P2X_2$ receptor channels, focusing especially on the correlation with the expression level. We compared the properties of the current evoked by a saturating dose

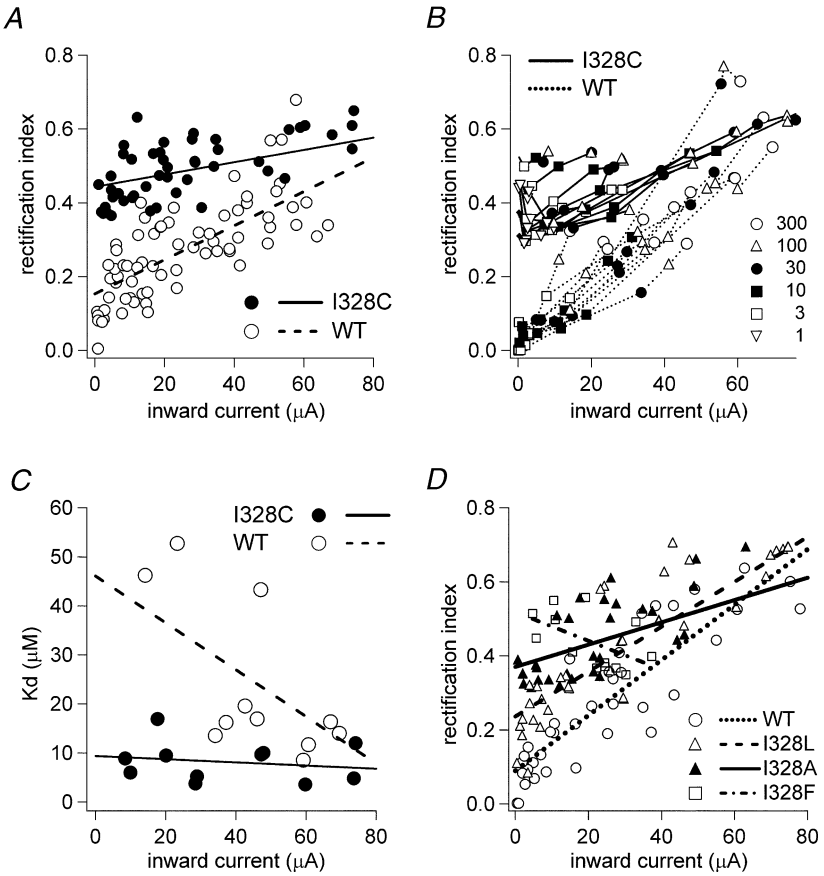


**Figure 6. Mutants altered the correlation between the inward rectification intensity and the expression density**
*A*, correlation between the rectification index ($I_{+40\ \mathrm{mV}}/I_{-60\ \mathrm{mV}}$) and the current amplitude. WT: ○ and dashed line; I328C mutant: ● and continuous line. *B*, accumulated data showing the correlation of the rectification index with the current amplitude evoked by various [ATP]. Symbols connected by lines are data from the same oocyte. WT: dotted lines; I328C: continuous lines. *C*, correlation between $K_d$ and the expression level. WT: ○ and dashed line; I328C: ● and continuous line. *D*, correlation between the rectification index ($I_{+40\ \mathrm{mV}}/I_{-60\ \mathrm{mV}}$) and the expression level. WT: ○; I328A: ▲; I328L: Δ and I328F: □. Calculated regression lines are also shown.

of ATP in oocytes with various expression levels, and observed that there is a strong correlation between the channel properties and the expression level, i.e. in oocytes with higher expression level, the inward rectification intensity of the evoked current was weaker, and the permeability of NMDG was higher.

### Dynamic changes of channel properties by mutual interaction between open channels

When we applied low [ATP] to oocytes with a high expression level, the inward rectification of the evoked current was strong, suggesting that the channel properties are not stable but can change dynamically in an open channel density-dependent manner. Virginio *et al.* (1999) have also reported a related finding that the pore dilatation of the $P2X_2$ receptor could occur more easily by applying higher [ATP]. The schematic drawing shown in Fig. 7 summarizes the dynamic changes in $P2X_2$ pore properties correlated with expression density and [ATP]. This scheme is based on the aforementioned 'mixed population model', and the explanation of the scheme is as follows. Open $P2X_2$ receptor channels exist as a mixture of two pore types, $O_1$ and $O_2$. Isolated open pores at low expression density or those activated by applying a low [ATP] are in the $O_1$ state, which shows strong rectification and low permeability to NMDG. The distances between open channels are reduced by increasing the expression level or by applying a higher [ATP]. Interactions between the open channels lead to a shift to the $O_2$ state, which shows weak rectification. Depending on the time after ATP application, the channels then shift further to the $O_3$ state, enabling permeation of NMDG. In contrast to the weak inward rectification property, the high NMDG permeability was achieved in a time-dependent manner after ATP application at high expression level. Therefore we think changes in the rectification property and the NMDG permeability are separable rather than go hand-in-hand.

The key point of this scheme is that interactions between open $P2X_2$ channels induce changes of pore properties. There are some preceding reports which go with this speculation. (1) Ding & Sachs (2002) analysed the single channel properties of the $P2X_2$ receptor in membrane patches containing one, two or three channels, and observed that the mean open time of multiple channels is much longer than that of an isolated channel; moreover, the open channel noise is lower in multiple channel patches than in patches with an isolated channel. This means

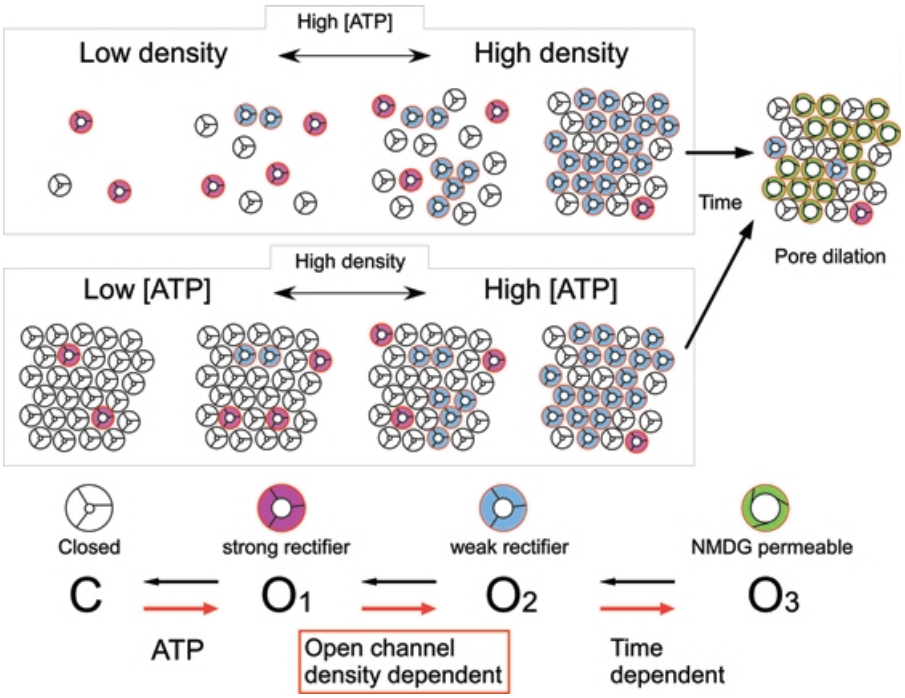


**Figure 7. Schematic drawings explaining the dynamic variation of inward rectification intensity depending on the open channel density**

The equilibrium is inclined toward the $O_2$ state, depending on the open channel density. $O_1$: a state showing a strong inward rectification and a low permeability to NMDG. $O_2$: a state showing no inward rectification. $O_3$: a state showing a high permeability to NMDG.

that the single channel properties differ depending on whether it is alone or in a group. (2) It is known that $P2X_2$ channels inhibit the activities of other ligand-gated channels. When $P2X_2$ receptors were coexpressed with other ionotropic receptors such as the nACh (Nakazawa, 1994; Khakh *et al.* 2000), $GABA_A$ (Sokolova *et al.* 2001) or $5HT_3$ (Barajas-Lopez *et al.* 2002) receptor, and were coactivated by applying both ligands, the amplitudes of the evoked current were smaller than the sum of the current amplitudes when the channels were activated individually. This was especially true when the expression level $P2X_2$ receptor was high (Khakh *et al.* 2000). These reports are compatible with our hypothesis that adjacent open $P2X_2$ channels are not independent of one another.

### Mechanistic insights for the density-dependent changes

It is noteworthy that the model we proposed in Fig. 7 has a similarity with the alamethicin model. Alamethicin is a channel pore-forming antibiotic, known to change its conductance levels with the increase in the concentration of channel monomer. This phenomenon is reported to be caused by the increase in the chance of collision and by the ensuing changes of the number of multimeric units (Sansom, 1993; Tieleman *et al.* 2002). These reports suggest a general mechanism of homophilic interaction between channels on the membrane, which could be also applied to the $P2X_2$ receptor channel.

It is of interest to estimate the density or the distance between $P2X_2$ channels at 'high' expression level, to determine if intermolecular interaction on the membrane could actually occur. With an assumption that the distribution on the membrane is uniform, we roughly estimated the density on the membrane surface. Using a single channel conductance, an open probability (Ding & Sachs, 1999) and an oocyte diameter ($\sim$1.1 mm), we obtained a value of as low as $\sim$25 channels $\mu m^{-2}$ on the membrane of oocytes with a high expression level, which is apparently lower than in the image drawn in Fig. 7. Since the membrane surface was shown not to be full of $P2X_2$ channel proteins, direct interaction does not seem to occur. However, if the channels do not sit still but float around on the membrane, there could be a good chance for the accidental collision and interaction of the molecules to occur at relatively high expression density. Also, if the channels are not expressed evenly, but clustered at hot spots with a very high local density, the intermolecular interaction could occur there. This possibility includes an accumulation of receptors by scaffold proteins and/or by lipid rafts. Based on these two reasons, it seems there remains a possibility that a direct interaction could occur.

To examine the possibility that $P2X_2$ receptors are clustered on the raft and that functional modulation by interaction occur there, we examined the effects of fumonisin B or $\beta$-cyclodextrin, which are known to destroy rafts by affecting sphingolipids or cholesterol, respectively. We also examined the effects of nocodazole or colchicine, which are known to disrupt microtubules, assuming that the cytoskeleton plays a critical role in the channel clustering. However, all these drugs did not influence the density-dependent changes of the inward rectification intensity of $P2X_2$ receptors (data not shown). Therefore, we could not obtain evidences that the high local density and interaction at the raft is critical in *Xenopus* oocytes.

In summary, the expression density on the membrane is not as high as shown in Fig. 7 on the assumption that the distribution is uniform. However, if we assume a diffusion of the receptor on the membrane and a presence of hot spots, there seems to be a good chance for direct interaction. As there is no strong evidence for or against this possibility, this point remains to be elucidated considering other possibilities also.

If $P2X_2$ 'ionotropic' receptor activation links to a 'metabotropic' pathway, it might be the mechanism of activated receptor density-dependent changes of channel properties. However, we think this possibility is very unlikely as there have been no preceding reports which showed metabotropic coupling of $P2X_2$ receptor activation, although it has been reported for the AMPA-type glutamate receptor as an exceptional case (Wang *et al.* 1997; Hayashi *et al.* 1999).

### Structural determinant for the density-dependent changes

What is the structural determinant for the density-dependent changes of the pore properties? We identified I328 as a critical site, which has been reported to be located in the second transmembrane region and to possibly contribute to the aqueous pore by Cys-scanning mutagenesis studies (Rassendren *et al.* 1997; Egan *et al.* 1998; Jiang *et al.* 2001). We observed that mutations of I328 to other amino acid residues significantly altered the slope of the correlation between the inward rectification intensity and the expression level; the rectification intensity of the I328C or I328A mutant was weak and changed only slightly with the increase in the expression level or in the ATP dose. It is noteworthy that mutations of I328 to small amino acid residues such as Ala and Cys induced clear changes. These results suggest that the pore structures of these mutants correspond to that of WT under the high expression density.

Judging from the location of I328 at the extracellular mouth of the pore, we speculate that it is not a site to detect the channel density information but a critical pore-forming or -modifying site influenced by the channel density, which affects channel properties such as inward rectification. Which other domain is then involved in the detection of the expression density? Eickhorst *et al.* (2002) reported that cytoplasmic C-terminal domains of $P2X_2$ controlled permeation of NMDG. To examine if this C-terminal cytoplasmic chain is important for the density-dependent changes of pore properties, we made a deletion mutant (R371stop) of the cytoplasmic region. The mutation, however, did not affect the correlation between the rectification intensity and the expression level. We speculate that C-terminus cytoplasmic domains of $P2X_2$ receptors are important for the transition from state $O_2$ to state $O_3$, but not from state $O_1$ to state $O_2$.

As there are some assumptions in the interpretation of the results of the Cys-scan mutagenesis, there remains a possibility that I328 does not actually face the permeation pathway (Rassendren *et al.* 1997). It is possible I328 mutation caused the observed changes in the present study by secondary effects on the pore structure or by affecting gating. In any case, we showed that mutations at I328 affected critically the expression level-dependent changes of the channel pore properties, although we do not know yet the mechanisms of homophilic interaction from the structural point of view.

### Significance in neurotransmission

It is needless to say that receptor properties such as rectification and ion permeability affect synaptic transmission significantly. For example, it was reported that synaptic transmissions are modulated by the strong inward rectification through neuronal nACh receptors (Sargent, 1993) or by the $Ca^{2+}$ permeation through NMDA-type glutamate receptors (Malenka & Nicoll, 1999). We therefore think that the open channel density-dependent changes of channel properties could serve as a very important modulation mechanism of synaptic function. The presence of various scaffold proteins could elevate the local density of receptors to a very high level, and the turnover of the scaffold proteins could induce fluctuation of the channel density. The density-dependent change of channel properties is not specific to $P2X_2$ receptors but also observed for voltage-gated channels. Honore *et al.* (1992) reported the inactivation properties and blocker sensitivity of the Shaker $K^+$ channel changed significantly depending on the expression level in *Xenopus* oocytes (Honore *et al.* 1992). Shaker $K^+$ channels are also known to show dynamic changes of ion selectivity during activation (Starkus *et al.* 1997) and C-type inactivation (Zheng & Sigworth, 1997). These reports support the possibility that that the density-dependent modulation we observed for the $P2X_2$ receptor can apply in general to receptors and channels at synaptic sites. Taken together, we think there is a good possibility the modulation of synaptic function could actually occur by open channel density-dependent changes of the properties of receptors and channels.

## References

Barajas-Lopez C, Montano LM & Espinosa-Luna R (2002). Inhibitory interactions between 5-HT3 and P2X channels in submucosal neurons. *Am J Physiol Gastrointest Liver Physiol* **283**, G1238–G1248.

Brake AJ, Wagenbach MJ & Julius D (1994). New structural motif for ligand-gated ion channels defined by an ionotropic ATP receptor. *Nature* **371**, 519–523.

Clyne JD, Brown TC & Hume RI (2003). Expression level dependent changes in the properties of P2X2 receptors. *Neuropharmacology* **44**, 403–412.

Ding S & Sachs F (1999). Single channel properties of P2X2 purinoceptors. *J General Physiol* **113**, 695–720.

Ding S & Sachs F (2002). Evidence for non-independent gating of P2X2 receptors expressed in *Xenopus* oocytes. *BMC Neurosci* **3**, 17.

Doyle DA, Morais Cabral J, Pfuetzner RA, Kuo A, Gulbis JM, Cohen SL, Chait BT & MacKinnon R (1998). The structure of the potassium channel: molecular basis of $K^+$ conduction and selectivity. *Science* **280**, 69–77.

Edwards FA, Gibb AJ & Colquhoun D (1992). ATP receptor-mediated synaptic currents in the central nervous system. *Nature* **359**, 144–147.

Egan TM, Haines WR & Voigt MM (1998). A domain contributing to the ion channel of ATP-gated P2X2 receptors identified by the substituted cysteine accessibility method. *J Neurosci* **18**, 2350–2359.

Eickhorst AN, Berson A, Cockayne D, Lester HA & Khakh BS (2002). Control of $P2X_2$ channel permeability by the cytosolic domain. *J General Physiol* **120**, 119–131.

Evans RJ, Derkach V & Surprenant A (1992). ATP mediates fast synaptic transmission in mammalian neurons. *Nature* **357**, 503–505.

Evans RJ, Lewis C, Virginio C, Lundstrom K, Buell G, Surprenant A & North RA (1996). Ionic permeability of, and divalent cation effects on, two ATP-gated cation channels (P2X receptors) expressed in mammalian cells. *J Physiol* **497**, 413–422.

Fujiwara Y & Kubo Y (2002). Ser165 in the second transmembrane region of the Kir2.1 channel determines its susceptibility to blockade by intracellular $Mg^{2+}$. *J General Physiol* **120**, 677–693.

Gu JG & MacDermott AB (1997). Activation of ATP P2X receptors elicits glutamate release from sensory neuron synapses. *Nature* **389**, 749–753.

Hayashi T, Umemori H, Mishina M & Yamamoto T (1999). The AMPA receptor interacts with and signals through the protein tyrosine kinase Lyn. *Nature* **397**, 72–76.

Honore E, Attali B, Romey G, Lesage F, Barhanin J & Lazdunski M (1992). Different types of $K^+$ channel current are generated by different levels of a single mRNA. *EMBO J* **11**, 2465–2471.

Jiang LH, Rassendren F, Spelta V, Surprenant A & North RA (2001). Amino acid residues involved in gating identified in the first membrane-spanning domain of the rat $P2X_2$ receptor. *J Biol Chem* **276**, 14902–14908.

Kato F & Shigetomi E (2001). Distinct modulation of evoked and spontaneous EPSCs by purinoceptors in the nucleus tractus solitarii of the rat. *J Physiol* **530**, 469–486.

Khakh BS (2001). Molecular physiology of P2X receptors and ATP signalling at synapses. *Nat Rev Neurosci* **2**, 165–174.

Khakh BS, Bao XR, Labarca C & Lester HA (1999). Neuronal P2X transmitter-gated cation channels change their ion selectivity in seconds. *Nat Neurosci* **2**, 322–330.

Khakh BS & Henderson G (1998). ATP receptor-mediated enhancement of fast excitatory neurotransmitter release in the brain. *Mol Pharmacol* **54**, 372–378.

Khakh BS, Humphrey PP & Surprenant A (1995). Electrophysiological properties of P2X-purinoceptors in rat superior cervical, nodose and guinea-pig coeliac neurones. *J Physiol* **484**, 385–395.

Khakh BS & Lester HA (1999). Dynamic selectivity filters in ion channels. *Neuron* **23**, 653–658.

Khakh BS, Smith WB, Chiu CS, Ju D, Davidson N & Lester HA (2001). Activation-dependent changes in receptor distribution and dendritic morphology in hippocampal neurons expressing P2X2-green fluorescent protein receptors. *Proc Natl Acad Sci USA* **98**, 5288–5293.

Khakh BS, Zhou X, Sydes J, Galligan JJ & Lester HA (2000). State-dependent cross-inhibition between transmitter-gated cation channels. *Nature* **406**, 405–410.

Kubo Y & Murata Y (2001). Control of rectification and permeation by two distinct sites after the second transmembrane region in Kir2.1 $K^+$ channel. *J Physiol* **531**, 645–660.

Malenka RC & Nicoll RA (1999). Long-term potentiation – a decade of progress? *Science* **285**, 1870–1874.

Nakazawa K (1994). ATP-activated current and its interaction with acetylcholine-activated current in rat sympathetic neurons. *J Neurosci* **14**, 740–750.

Nichols CG & Lopatin AN (1997). Inward rectifier potassium channels. *Annu Rev Physiol* **59**, 171–191.

Nicke A, Baumert HG, Rettinger J, Eichele A, Lambrecht G, Mutschler E & Schmalzing G (1998). P2X1 and P2X3 receptors form stable trimers: a novel structural motif of ligand-gated ion channels. *EMBO J* **17**, 3016–3028.

Nishida M & MacKinnon R (2002). Structural basis of inward rectification: cytoplasmic pore of the G protein-gated inward rectifier GIRK1 at 1.8 A resolution. *Cell* **111**, 957–965.

North RA (2002). Molecular physiology of P2X receptors. *Physiol Rev* **82**, 1013–1067.

North RA & Barnard EA (1997). Nucleotide receptors. *Curr Opin Neurobiol* **7**, 346–357.

Rassendren F, Buell G, Newbolt A, North RA & Surprenant A (1997). Identification of amino acid residues contributing to the pore of a P2X receptor. *EMBO J* **16**, 3446–3454.

Sansom MS (1993). Alamethicin and related peptaibols – model ion channels. *Eur Biophys J* **22**, 105–124.

Sargent PB (1993). The diversity of neuronal nicotinic acetylcholine receptors. *Annu Rev Neurosci* **16**, 403–443.

Sokolova E, Nistri A & Giniatullin R (2001). Negative cross talk between anionic $GABA_A$ and cationic P2X ionotropic receptors of rat dorsal root ganglion neurons. *J Neurosci* **21**, 4958–4968.

Starkus JG, Kuschel L, Rayner MD & Heinemann SH (1997). Ion conduction through C-type inactivated Shaker channels. *J General Physiol* **110**, 539–550.

Surprenant A, Rassendren F, Kawashima E, North RA & Buell G (1996). The cytolytic P2Z receptor for extracellular ATP identified as a P2X receptor (P2X7). *Science* **272**, 735–738.

Tieleman DP, Hess B & Sansom MS (2002). Analysis and evaluation of channel models: simulations of alamethicin. *Biophys J* **83**, 2393–2407.

Valera S, Hussy N, Evans RJ, Adami N, North RA, Surprenant A & Buell G (1994). A new class of ligand-gated ion channel defined by P2x receptor for extracellular ATP. *Nature* **371**, 516–519.

Virginio C, MacKenzie A, Rassendren FA, North RA & Surprenant A (1999). Pore dilation of neuronal P2X receptor channels. *Nat Neurosci* **2**, 315–321.

Wang Y, Small DL, Stanimirovic DB, Morley P & Durkin JP (1997). AMPA receptor-mediated regulation of a Gi-protein in cortical neurons. *Nature* **389**, 502–504.

Zheng J & Sigworth FJ (1997). Selectivity changes during activation of mutant Shaker potassium channels. *J General Physiol* **110**, 101–117.

Zhou Z & Hume RI (1998). Two mechanisms for inward rectification of current flow through the purinoceptor P2X2 class of ATP-gated channels. *J Physiol* **507**, 353–364.

Zhou Y, Morais-Cabral JH, Kaufman A & MacKinnon R (2001). Chemistry of ion coordination and hydration revealed by a $K^+$ channel-Fab complex at 2.0 A resolution. *Nature* **414**, 43–48.

## Acknowledgements

We are grateful to Dr D. Julius (University of California, San Francisco) for providing us with $P2X_2$ cDNA. This work was supported partly by research grants from the Ministry of Education, Science, Sports, Culture, and Technology of Japan and from foundations of Novartis and Salt Science.